Immune and Genetic Signatures of Breast Carcinomas Triggering Anti-Yo–Associated Paraneoplastic Cerebellar Degeneration

Elise Peter, Isabelle Treilleux, Valentin Wucher, Emma Jougla, Alberto Vogrig, Daniel Pissaloux, Sandrine Paindavoine, Justine Berthet, Géraldine Picard, Véronique Rogemond, et al.

HAL Id: hal-03915422
https://hal.inria.fr/hal-03915422

Submitted on 29 Dec 2022

Immune and Genetic Signatures of Breast Carcinomas Triggering Anti-Yo–Associated Paraneoplastic Cerebellar Degeneration

Elise Peter, MSc, Isabelle Treilleux, MD, PhD,* Valentin Wucher, PhD,* Emma Jougla, MSc, Alberto Vogrig, MD, Daniel Pissaloux, PhD, Sandrine Paindavoine, PhD, Justine Berthet, MSc, Géraldine Picard, Véronique Rogemond, PhD, Marine Villard, Clémentine Vincent, PhD, Laurie Tonon, PhD, Alain Viari, PhD, Jérôme Honnorat, MD, PhD, Bertrand Dubois, PhD, and Virginie Desestret, MD, PhD

Correspondence
Dr. Desestret
virginie.desestret@chu-lyon.fr

Abstract

Background and Objectives

Paraneoplastic cerebellar degeneration (PCD) with anti-Yo antibodies is a cancer-related autoimmune disease directed against neural antigens expressed by tumor cells. A putative trigger of the immune tolerance breakdown is genetic alteration of Yo antigens. We aimed to identify the tumors' genetic and immune specificities involved in Yo-PCD pathogenesis.

Methods

Using clinicopathologic data, immunofluorescence (IF) imaging, and whole-transcriptome analysis, 22 breast cancers (BCs) associated with Yo-PCD were characterized in terms of oncologic characteristics, genetic alteration of Yo antigens, differential gene expression profiles, and morphofunctional specificities of their in situ antitumor immunity by comparing them with matched control BCs.

Results

Yo-PCD BCs were invasive carcinoma of no special type, which early metastasized to lymph nodes. They overexpressed human epidermal growth factor receptor 2 (HER2) but were hormone receptor negative. All Yo-PCD BCs carried at least 1 genetic alteration (variation or gain in copy number) on *CDR2L*, encoding the main Yo antigen that was found aberrantly overexpressed in Yo-PCD BCs. Analysis of the differentially expressed genes found 615 upregulated and 54 downregulated genes in Yo-PCD BCs compared with HER2-driven control BCs without PCD. Ontology enrichment analysis found significantly upregulated adaptive immune response pathways in Yo-PCD BCs. IF imaging confirmed an intense immune infiltration with an overwhelming predominance of immunoglobulin G–plasma cells.

Discussion

These data confirm the role of genetic alterations of Yo antigens in triggering the immune tolerance breakdown but also outline a specific biomolecular profile in Yo-PCD BCs, suggesting a cancer-specific pathogenesis.

Glossary

BC = breast cancer; **CDR2** = cerebellar degeneration-related protein 2; **CGHa** = comparative genomic hybridization array; **CNV** = copy number variation; **COSMIC** = Catalogue Of Somatic Mutations In Cancer; **DCIS** = ductal carcinoma in situ; **ECM** = extracellular matrix; **FFPE** = formalin-fixed paraffin-embedded; **GO** = Gene Ontology; **HER2** = human epidermal growth factor receptor 2; **HR** = hormone receptor; **IF** = immunofluorescence; **IgG** = immunoglobulin G; **IHC** = immunohistochemistry; **MCP** = Microenvironment Cell Populations; **mDC** = myeloid dendritic cell; **NST** = no special type; **OBC** = occult BC; **OR** = estrogen receptor; **PCD** = paraneoplastic cerebellar degeneration; **PR** = progesterone receptor.

Paraneoplastic cerebellar degeneration (PCD) is a rare condition but is one of the commonest paraneoplastic neurologic disorders, mainly associated with breast and ovarian carcinomas.[1] The main feature is a rapidly progressive cerebellar ataxia secondary to the specific destruction of Purkinje cells by cytotoxic T cells.[2,3] About 50% of PCD cases are associated with anti-Yo autoantibodies (Yo-PCD), directed against Yo antigens CDR2 (cerebellar degeneration-related protein 2) and its paralogue CDR2L.[4-6] The previous description of an uncommon and intense immune attack in Yo-PCD ovarian cancers[7] highlighted that antitumor immunity has a lead role in paraneoplastic syndrome pathogenesis. The presence of specific alterations of genes encoding Yo antigens (copy number gain leading to antigen overexpression and somatic sequence variations) in all Yo-PCD ovarian cancers strongly suggests that neoantigenicity is a pivotal mechanism leading to the immune tolerance breakdown that could in turn drive the immune overreaction spearheading the paraneoplastic syndrome. Hypothesizing the aforementioned Yo gene specificities to be causative in immune tolerance breakdown in Yo-PCD, similar genetic alterations should be found in breast cancer (BC) associated with Yo-PCD. However, the already described overexpression of human epidermal growth factor receptor 2 (HER2) in Yo-PCD BCs[8] leads to believe that antigen specificities are not the only molecular triggers of the immune tolerance breakdown and that other mechanisms, potentially linked to breast oncogenesis, could be involved. To move forward in our understanding of the mechanisms leading to this specific immune reaction, we analyzed the salient clinical, histopathologic, and immunologic features, gene expression profiles, and mutational status of Yo-PCD BCs.

Methods

Patients

Patients with Yo-PCD and a BC diagnosed between January 2005 and March 2021 were identified retrospectively by the French Reference Center for Paraneoplastic Neurological Syndromes (Lyon, France). Patients were included if they had (1) PCD diagnosis according to the international guidelines,[9] (2) presence of Yo antibodies in serum and/or CSF detected using both immunohistochemistry (IHC) on rat brain sections and dot blot using commercial tests (RAVO diagnostika and Euroimmun), and (3) histologically proven BC.

From those included, tumor samples were retrieved when available. Of note, for patients with several nonconcomitant tumors (e.g., patients who had several successive BCs) or tumor sites (e.g., primary BC and lymph node metastasis), we chose—whenever possible—to include all available tumor samples. In this way, we aimed to take into account the potential asynchronism of cancer and PCD onset, and thus, the impossibility to know a priori which tumor sample was responsible for PCD triggering when patients had had several BCs but also the possibility of a "cumulative effect" of different tumors in the same patients. Accordingly, when the primitive tumor and lymph node metastasis were available, we chose to include both samples, as it was possible that only 1 of the 2 tumor sites was responsible for paraneoplastic syndrome pathogenesis. This raise the possibility of potential duplicates or triplicates in the analysis that were systematically taken into account in interpretation of results.

Control Specimens

A cohort of 15 BCs without Yo-PCD from the Biopathology Department of Centre Léon Bérard (Lyon, France) was constituted matched with Yo BCs on their pathologic type and expression of HER2 and hormone receptor (HR).

Tumor Pathology Study

Four-μm-thick formalin-fixed paraffin-embedded (FFPE) tissue sections were stained with hematoxylin-phloxine-saffron. A referent pathologist (I.T.) assessed the subtype of BCs according to the 2019 WHO classification.[10]

Immunohistochemistry

Detailed chromogen IHC protocols and antibodies are described in the eMethods (links.lww.com/NXI/A734). Classical diagnostic markers including estrogen (OR) and progesterone (PR) receptors were obtained by a routine automated protocol. HER2 expression was assessed using prediluted monoclonal anti-HER2 antibody 4B5 (Roche Diagnostics, Basel, Switzerland). CDR2L expression was assessed using an automated IHC protocol. A staining intensity value from 0 (no staining) to 3 (high staining) was given by manual quantification conducted by 2 evaluators blinded to the provenance (patient or control) of the sample.

Multiplex Immunofluorescence Tissue Staining and Digital Image Analysis

Multispectral IF Tissue Imaging

Eight Yo-PCD BC samples were compared with 14 HER2-driven control BC samples. Fully automated seven-color multiplex immunofluorescence (IF) was performed using the Opal system (Akoya Biosciences, Marlborough, MA) and the BOND

Table 1 Clinicopathologic Description of the Yo-PCD BC Cohort

Tumor characteristics		34 BCs, n (%)
Pathology		
	Invasive carcinomas of NST	31 (91.1)
	Intragalactophoric carcinoma	2 (5.8)
	Medullary carcinoma	1 (2.9)
Nottingham grade		
	III	19 (55.9)
	II	6 (17.6)
	NA	9 (26.5)
Tumor subtype		
	HER2− hormone receptor +	2 (5.8)
	HER2+ hormone receptor +	6 (17.6)
	HER2+ hormone receptor −	23 (67.6)
	TNBC	3 (8.8)
Receptor expression		
	OR	7 (20.6)
	PR	5 (14.7)
	HER2	29 (85.3)
Tumor size		
	T0	7 (20.6)
	Tis	3 (8.8)
	T1	10 (29.4)
	T2	8 (23.5)
	T3	3 (8.8)
	Tx	3 (8.8)
Lymph node metastasis		
	N0	9 (26.5)
	N+	23 (67.6)
	NA	2 (5.8)
No. of cancer diagnosed per patient (n = 29 patients)	3 cancers	1 (3.4)
	2 cancers	3 (10.3)
	1 cancer	25 (86.2)

Abbreviations: HER2 = ErbB2 protein; NA = not available; NST = no specific type; OR = estrogen receptor; PR = progesterone receptor; TNBC = triple-negative breast carcinoma; TNM = tumor node metastasis.
Nottingham grade is a composite pathologic prognostic score taking into account differentiation, atypia, and mitotic activity ranging from grade 1 (best prognosis) to 3 (worse prognosis); TNM staging: T0: no detectable tumor, Tis: in situ tumor, T1: tumor is ≤2 cm across, T2: tumor is >2 cm but ≤5 cm across, T3: tumor is >5 cm across, N0: no cancer cell in any lymph node, N+: cancer cells in at least 1 lymph node.

RX stainer (Leica Biosystems, Nanterre, France) for patients with available FFPE tumor tissue. The sections were sequentially stained with each primary antibody, followed by OPAL-Horseradish Peroxidase secondary antibody incubation then revealed in the following order: DClamp (dendritic cell lysosomal-associated membrane glycoprotein), CD 20, immunoglobulin (Ig)G, IgA, CD3, and cytokeratin. The sections were then counterstained with spectral 4′,6-diamidino-2-phenylindole and mounted with a coverslip. Detailed IF protocols and antibodies are described in the eMethods (links.lww.com/NXI/A734).

Quantification of Immune Cell Densities

Representative regions of interests (6 for tissue <100 mm², 10 otherwise) were defined on whole-slide digital images using the Phenochart software v. 1.0.12 (Akoya Biosciences). After cell segmentation using 4′,6-diamidino-2-phenylindole, the different immune cell phenotypes were quantified, and data were processed on phenoptrReports v.0.2.10 R package (Akoya Biosciences) to obtain cell densities.

RNA Sequencing

Fifteen of the 22 Yo-PCD BC samples were eligible for RNA-seq analysis (7 were discarded because of insufficient material or RNA extraction failure). Sequencing was performed (paired end, 2 × 75 cycles) using NextSeq 500/550 High Output V2 kit on a NextSeq 500 machine (Illumina, San Diego, CA). The mean number of reads per sample was around 80 millions. Alignments were performed using STAR[11] on the GRCh38 version of the human reference genome. The amount of duplicate reads were assessed using PICARD tools.[12] Samples with a number of unique reads below 10 million (5 million paired-reads) were discarded from the analysis. Expression values were extracted using Kallisto version 0.42.5 with GENECODE release 23-genome annotation based on the GRCh38 genome reference.

Comparative Genomic Hybridization Array

Comparative genomic hybridization array (CGHa; accession number in NCBI's Gene Expression Omnibus: GSE96039) was performed on 10 Yo-PCD BC samples. Fragmentation, labeling, cohybridization on 4 × 180 K Agilent SurePrint G3 Human whole-genome oligonucleotide arrays (Agilent Technologies), scanning, and analysis are fully described in the eMethods (links.lww.com/NXI/A734).

DNA Sequencing

CDR2 and *CDR2L* genes were sequenced on 8 Yo-PCD BC samples using the MiSeq next-generation sequencing platform (Illumina) according to the manufacturer's instructions and described in the eMethods (links.lww.com/NXI/A734). The sequence data generated were aligned using NextGENe (SoftGenetics, State College, PA) on human reference sequences hg38 for *CDR2* (NM_001802.1) and *CDR2L* (NM_014603.2).

Fluorescent In Situ Hybridization

Copy number alterations of the *CDR2L* gene were assessed on 12 Yo-PCD BC samples and 15 control BC samples with a

Table 2 Histologic and Biomolecular Characteristics of Yo-PCD BCs

Patient no.	Sample	Sample type	*ErbB2* CNV	HER2 IHC expression	OR	PR	PCD-cancer interval, mo	Genetic alteration on the *CDR2* or *CDR2L* gene	*CDR2L* CNV	*CDR2* CNV	CDR2L expression (IHC)
1	A	PBT	NA	−	+	+	44	None	None	NA	+
	B	PBT	Amplification	+++	0	0	6	p.R394Q (*CDR2L*)	None	None	+
	C	MLN	None	−	0	0	1	p.V176M (*CDR2*)	Gain	None	++
2		PBT	NA	++	0	0	24	NA	Amplification	NA	+++
3		PBT	Amplification	+++	0	0	−1	In-frame fusion CDR2L-CTD-2206N4.4	Amplification	None	+++
4		PBT	NA	+++	0	+	2	NA	NA	NA	+++
5	A	MLN	NA	++	0	0	152	NA	NA	NA	+
	B	MLN	NA	++	0	0	22	NA	NA	NA	++
6	A	PBT	NA	+++	+	0	−5	None	Amplification	NA	+++
	B	MLN	Amplification	+++	+	0	−5	None	Amplification	None	+++
7		PBT	NA	+++	0	0	6	NA	NA	NA	+++
8		PBT + MLN	NA	+++	0	0	1	NA	NA	NA	++
9		PBT	Amplification	+++	0	0	−1	p.Q50X (*CDR2L*)	Amplification	Gain	++
10		PBT	Amplification	+++	0	0	−5	NA	Amplification	None	+++
11		MLN	NA	+++	0	0	0	NA	NA	NA	++
12		PBT	None	−	0	0	105	p.R216W (*CDR2*)	Gain	None	−
13	A	PBT	None	−	+	+	8	None	None	Strong gain	+
	B	PBT	Amplification	+++	0	0	8	None	Amplification	Gain	+++
14		PBT	NA	−	0	0	111	p.S138L (*CDR2*)	NA	NA	++
15		MLN	Amplification	+++	0	0	−2	None	Amplification	None	+++
16		MLN	NA	+++	0	0	−2	NA	NA	NA	NA
17		PBT	NA	+++	0	0	3	NA	NA	NA	+++

Abbreviations: CNV = copy number variation; HER2 = ErbB2 protein; MLN = metastatic lymph node; NA = not available; OR = estrogen receptor; PBT = primary breast tumor; PCD = paraneoplastic cerebellar degeneration; PR = progesterone receptor.
The interval between PCD and cancer is calculated with cancer diagnosis as day 0; the negative interval thus corresponds to patients for whom PCD was diagnosed before cancer.

Figure 1 Flowchart of the Study
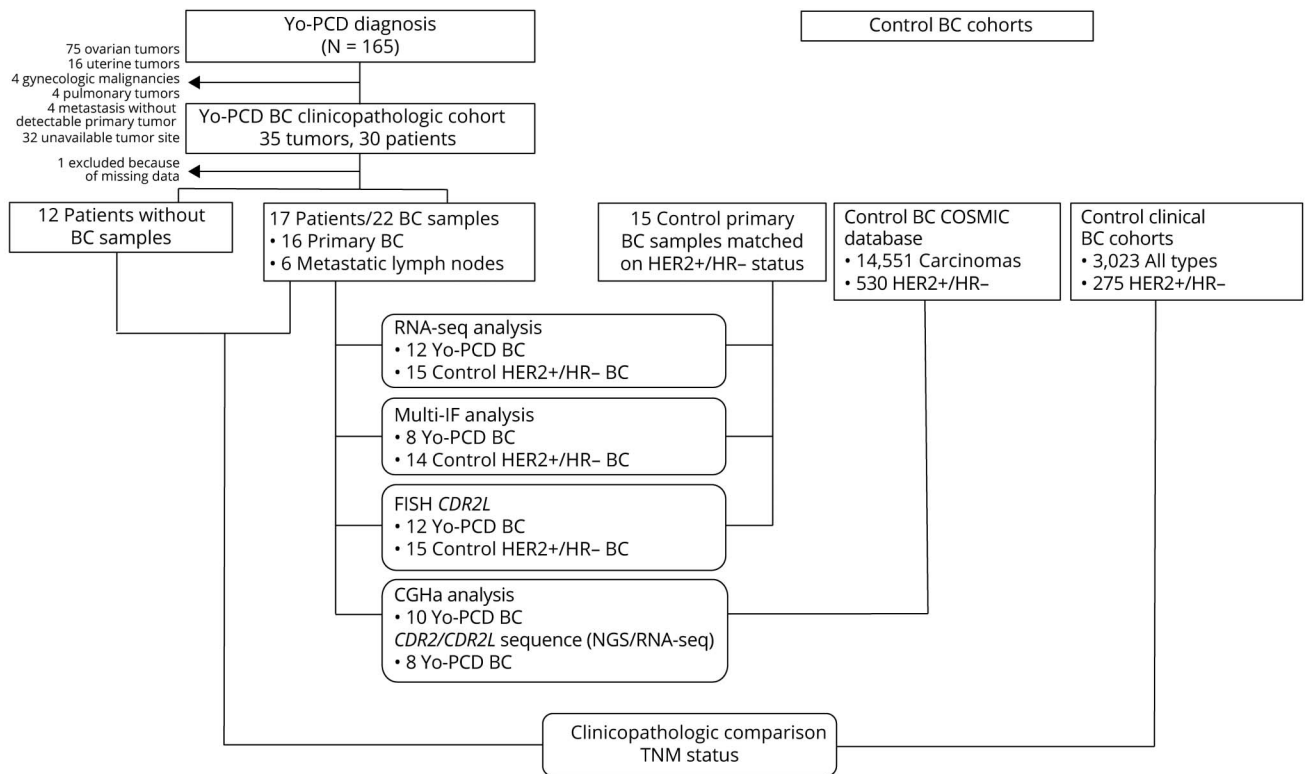
Control cohorts are (i) from in-house HER2-driven control tumors for the RNA-seq, multi-IF, and FISH analyses, (ii) from the COSMIC database[19] for the CGHa and the DNA sequencing of *CDR2* and *CDR2L*, or (iii) from a literature-drawn cohort[27] for the clinicopathologic comparison. BC = breast cancer; CGHa = comparative genomic hybridization array; FISH = fluorescent in situ hybridization; HER2+ = overexpression of human epidermal growth factor receptor 2; HR− = no overexpression of hormone receptors; PCD = paraneoplastic cerebellar degeneration; w/o = without.

dual color probe where the *CDR2L* gene is labeled in orange, and the centromere of chromosome 17 is labeled in green (Empire Genomics, Buffalo, NY). The *CDR2L* gene was considered amplified if the mean number of orange signals was ≥6.

Statistical and Bioinformatical Analysis

Statistical analysis was performed using R v.4.0.3.[13] Comparisons were made using the χ^2 or Fisher exact test according to preanalytical conditions. Cell densities evaluated with multi-IF were compared using the Mann-Whitney U test.

Bioinformatical analyses are detailed in the eMethods (links.lww.com/NXI/A734). Differential gene expression analysis was performed using DESeq2 v1.32.0[14] R package by comparing gene expression between Yo-PCD and controls. Hierarchical clustering was performed using the ComplexHeatmap v2.8.0[15] R package using the Euclidean distance and the Ward clustering method. Gene Ontology (GO) enrichment was performed using cluster-Profiler v4.0.0[16] R package on overexpressed and underexpressed Yo-PCD genes separately, and all genes used for differential gene expression were used as background. Immune cell populations were analyzed using the Microenvironment Cell Populations-counter (MCP-counter) method[17] and the MCPCounter v1.1 R package.

Study Approval

This study is part of the project Gene PNS (NCT03963700) and was approved by the institutional review board of the Hospices Civils de Lyon. Tumors and other biological samples were collected after patients gave informed and written consent.

Data Availability

RNA-seq expression, differential expression results, and GO enrichment analysis data are available online (zenodo.org/record/6477807, doi: 10.5281/zenodo.6477807). RNA-seq raw data (FASTQ) will be shared with any qualified investigator on request.

Results

Clinical and Pathologic Cohorts

Thirty patients with Yo-PCD associated with a BC were identified; 1 patient was excluded because of missing clinical data. For the 29 patients with Yo-PCD included, the histopathologic data of 34 BCs were collected (Table 1); 17 patients had available FFPE tissue samples: 6 axillary lymph nodes and 16 primary BCs. One patient had 3 available samples (patient 1), and 3 patients had 2 available samples (patients 5, 6, and 13); a total of
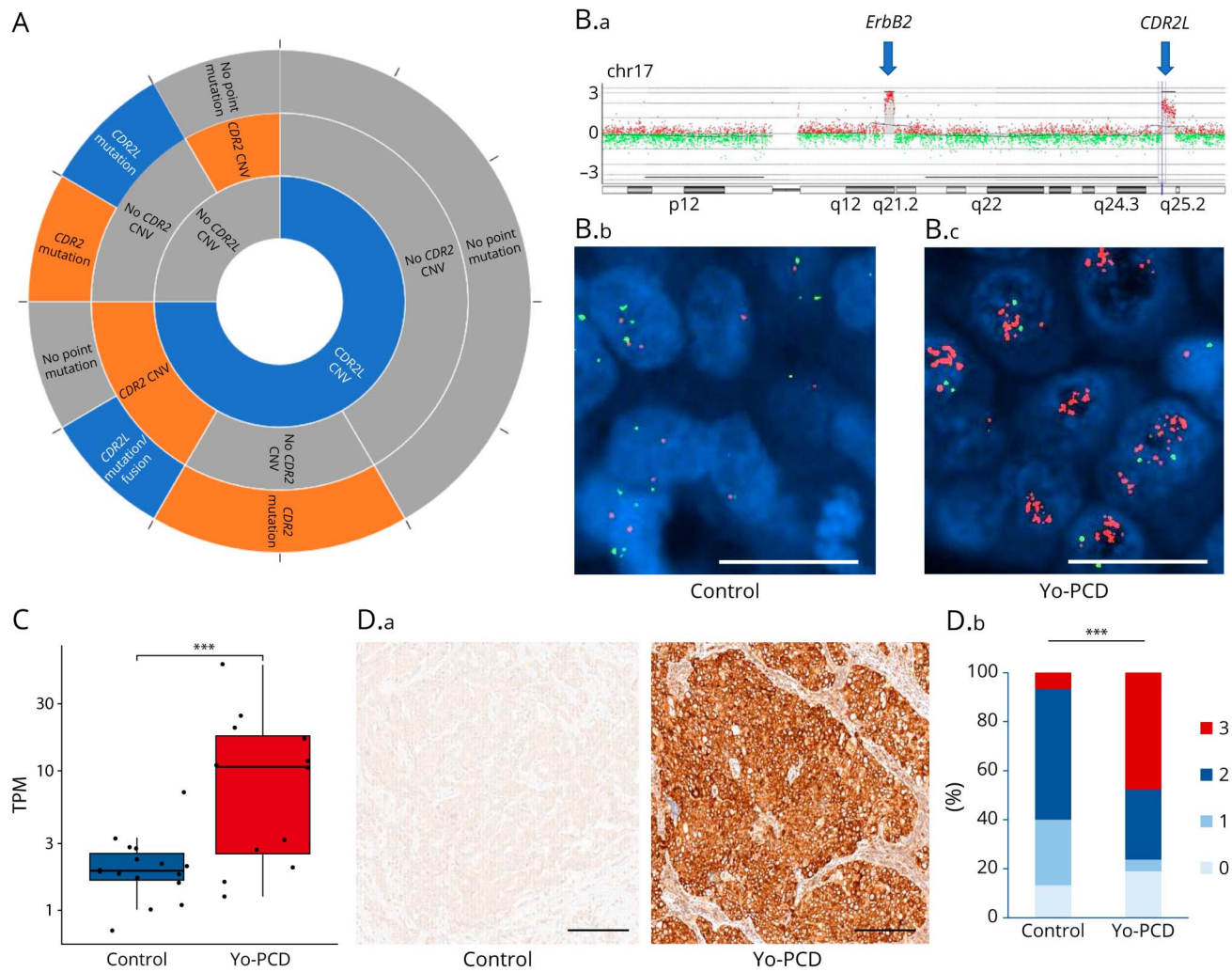
(A) Genetic alterations (mutations and copy number variations) in the *CDR2* (in orange) and *CDR2L* (in blue) locus. Each section of the circle represents 1 Yo-PCD breast cancer (BC); the inner circle shows *CDR2L* CNV, whereas *CDR2* CNV is represented in the intermediate circle. The outer circle gives information on point mutations and fusions on the *CDR2* or CDR2L locus. (B.a) Cytogenetic alterations on the CDR2L locus. (B.b) CGHa on Yo-PCD breast tumor: zoom on 17q chromosome holding ERBB2 (HER2) and CDR2L locus amplifications. (B.c) CDR2L-probe FISH in control breast cancer (left) vs Yo-PCD (right). Scale bar: 50 μm. (C) Median boxplots of TPM expression of CRD2L in control breast tumors (left, dark blue) vs Yo-PCD tumors (right, red). CDR2L was found differentially expressed in the RNA-seq analysis. (D.a and D.b) Expression of the CDR2L protein. (D.a) Representative CDR2L IHC staining in control breast tumors (left) vs Yo-PCD tumors (right). Scale bars: 100 μm. (D.b) Semiquantitative evaluation of CDR2L staining intensity in IHC in control breast tumors (left) vs Yo-PCD tumors (right) ranked from 0 for no staining (faded blue) to 3 for cytoplasmic staining with strong intensity (red). Comparison with the χ^2 independent test. PCD = paraneoplastic cerebellar degeneration.

22 samples were analyzed. Histologic data on each available tumor sample are detailed for each patient in Table 2, and the study flowchart summarizing the methods and analyses applied to characterize Yo-PCD BCs compared with control BCs is presented in Figure 1.

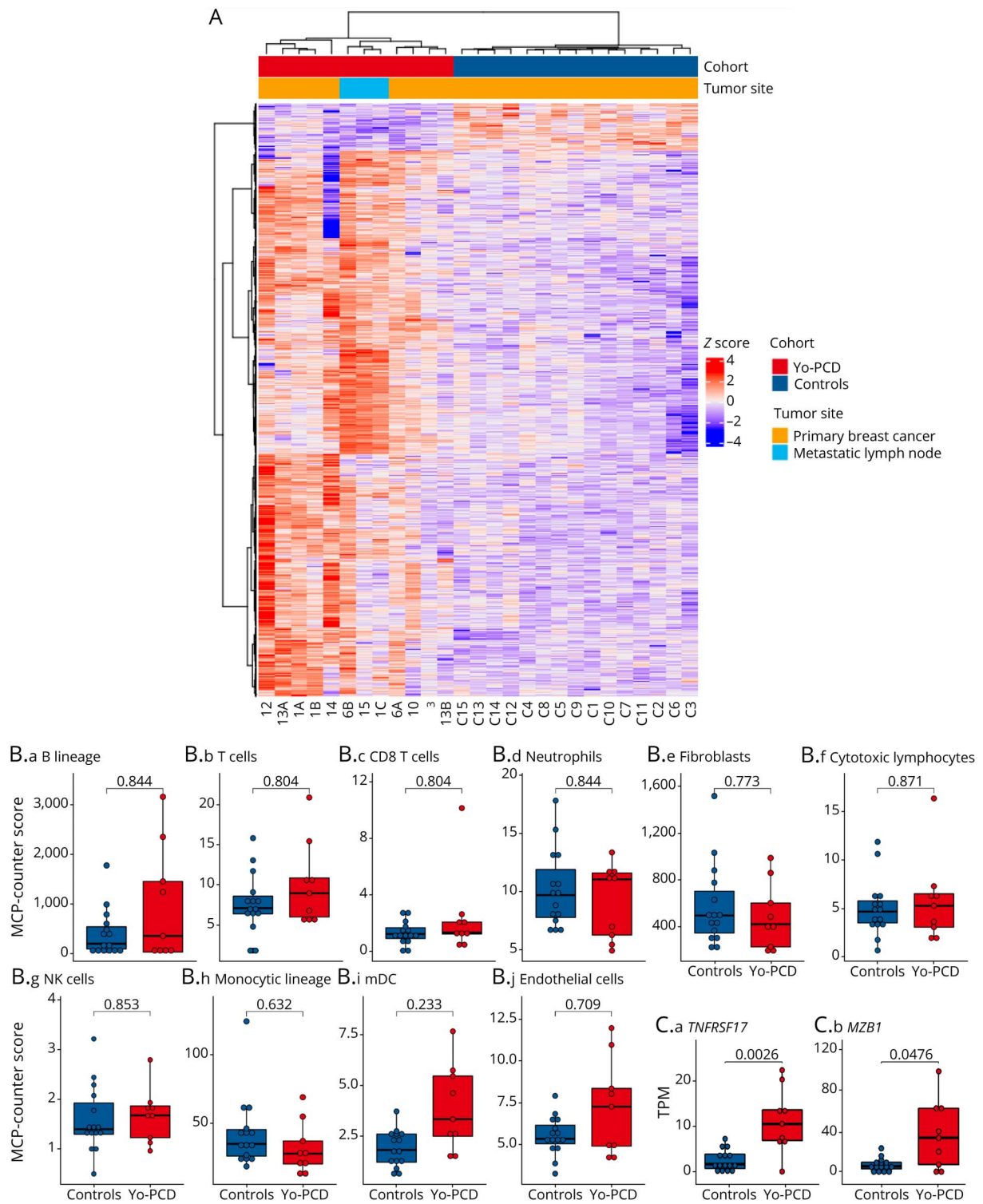## Yo-PCD BCs Are Mainly HER2-Positive and HR-Negative Invasive Carcinomas of No Special Type

Thirty-one of the 34 (91.1%) Yo-PCD BCs were invasive carcinomas of no special type (NST). The Nottingham grade[18] was available for 25 samples: 19 BCs were grade 3 (55.9%), and the other 6 were grade 2 (17.6%). IHC found that HER2 was overexpressed in 29 (85.3%) Yo-PCD BCs and amplification of *ErbB2*, encoding HER2, was found in 17

of 22 (77.2%). HRs, namely PR and OR, were both negative in 26 BCs (76.4%). Overall, the majority (67.6%) of Yo-PCD BCs were HER2-positive and HR-negative invasive carcinomas of NST, also called HER2-driven BCs (Table 1).

Yo-PCD BCs Are Small-Sized BCs Early Metastasizing in Regional Lymph Nodes

Overall, 20 of 34 (58.8%) Yo-PCD BCs were T1 or lower and 23 of 34 BCs (67.6%) had ipsilateral axillary lymph node metastasis at diagnosis (Table 1). Seven of the 34 BCs (20.5%) had an occult BC (OBC) with axillary lymph node metastasis for which a definitive pathologic diagnosis was obtained after lymph node biopsy without detection of any primary breast tumor following appropriate radioclinical

(A) Heatmap of the differentially expressed genes (in rows) between Yo-PCD (red) and control (dark blue) samples (in columns). Tumor sites are separated in primary breast cancer (BC; yellow) and metastatic lymph node (light blue). TPM expression values were first transformed into log10(TPM + 0.01) and then transformed into a Z score per gene. Panels B and C show boxplots of the median value and interquartile range (IQR) for the concerned variable of control (on the left, in blue) and Yo-PCD BC samples (on the right, in red); the upper whisker extends from the hinge to the largest value no further than 1.5 × IQR, and the lower whisker extends to the smallest value at most 1.5 × IQR from the hinge; each dot represents the value of a sample. *p* Values of comparisons between Yo-PCD and control groups using the Wilcoxon rank-sum test are adjusted with the Benjamini and Hochberg method (see eMethods for detail, links.lww.com/NXI/A734) and shown on the top of each couple of boxplots. Yo-PCD samples from metastatic lymph nodes have been removed. (B.a–B.j) Boxplots of MCP-counter estimates for 3 classical cell types in control and Yo-PCD samples. (C.a-b) Boxplots of TPM expression of 2 typical plasma cell markers in control and Yo-PCD samples. PCD = paraneoplastic cerebellar degeneration.

Figure 4 Multiplex Immunofluorescence and Immune Cell Densities
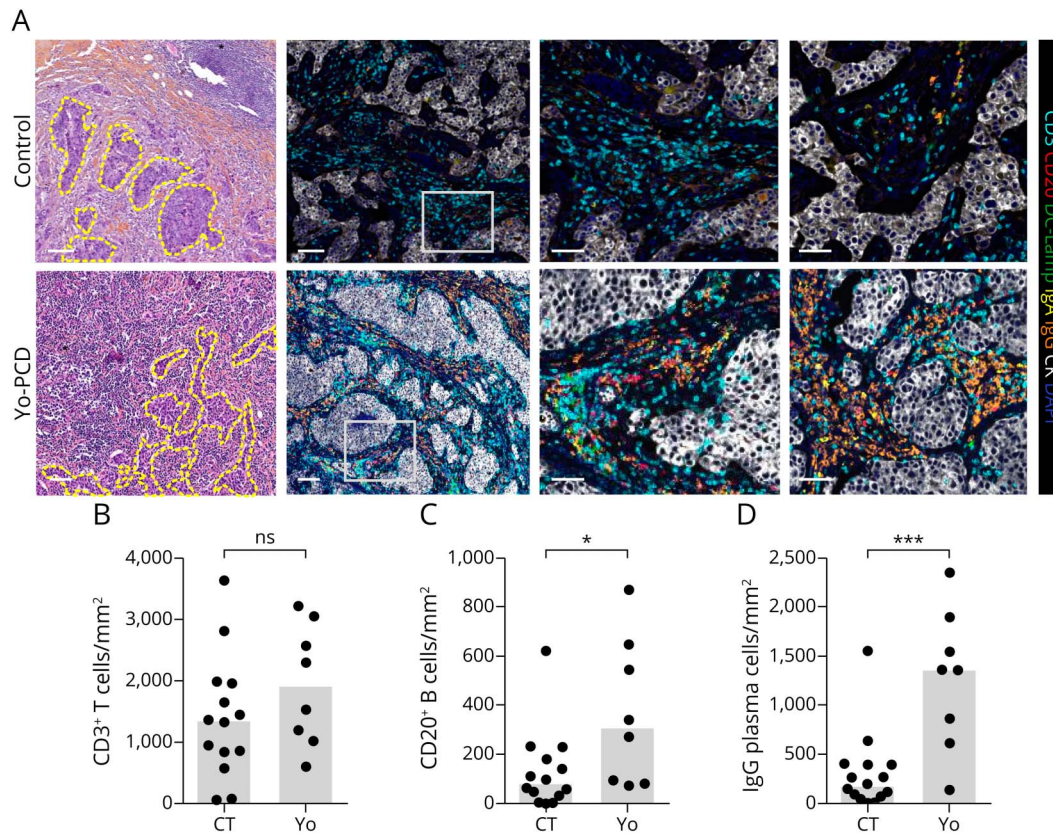
(A) Representative control and Yo-PCD breast cancer (BC) slides with (from left to right): hematoxylin-phloxine-saffron coloration at low magnification (tumor nests are circled by dotted yellow lines, scale bar: 200 μm), high magnification images illustrating the great density and variety of immune cells infiltrating Yo-PCD BCs as compared to control BCs, and representative multi-immunofluorescence slides of control and Yo-PCD BCs showing the B cells and massive IgG-plasma cells infiltration characterizing Yo-PCD BCs (scale bar: 100 μm). B to D: Represented plots show the median value (top of the gray rectangle) of the concerned variable. Each dot represents the value of a sample. p Values of comparisons between controls and Yo-PCD BCs using the Mann-Whitney method are shown at the top of each panel. B: Absolute counts of T cells/mm² in controls and Yo-PCD BCs. C: Absolute counts of B cells/mm² in controls and Yo-PCD BCs. D: Absolute counts of IgG plasma cells/mm² in controls and Yo-PCD BCs. CT = control tumors; PCD = paraneoplastic cerebellar degeneration.

assessment (including ad hoc nuclear imaging). Three patients only had ductal carcinoma in situ (DCIS), including 2 of 3 with axillary lymph node metastasis.

Yo Genes Are Mutated, Amplified, and Overexpressed in Yo-PCD BCs

As CDR2 and CDR2L are the targets of the anti-Yo antibodies, a first focus was made on these 2 proteins. The mutational status of Yo genes (*CDR2* and *CDR2L*) was assessed by DNA and/or RNA sequencing on 12 Yo-PCD BC samples from 8 different patients (1A, B, C; 3; 6A, B; 10; 12; 13A, B; 14; and 15). Sequence alterations were found in 6 Yo-PCD BCs (1B, 1C, 3, 9, 12, and 14; Table 2): 3 in *CDR2* (n = 3) and 3 in *CDR2L* including an in-frame fusion (Figure 2A). Only one of these variants (R216W, patient 12) has been reported in the Single-Nucleotide Polymorphism Catalogue Of Somatic Mutations In Cancer (COSMIC) database.[19] This, together with the absence of mutations in the matched constitutional counterpart (available for patients 3 and 9) and in the blood DNA of 10 patients with Yo-PCD without evaluable tumor tissue, indicated that these mutations were somatic.

Four of these mutations resulted in amino acid substitutions in the protein sequence, and 1 leads to protein truncation. Overall, 5 of 8 (62.5%) patients with Yo-PCD displayed at least 1 alteration in the *CDR2* or *CDR2L* gene.

Information on *CDR2L* CNV was available for 13 samples by CGHa and fluorescent in situ hybridization (FISH; n = 9), CGHa alone (n = 1), or FISH alone (n = 3), 8 of which displayed amplification (61.5%) and 2 had a significant gain in 17q25 carrying the *CDR2L* gene (Figure 2B). By contrast, amplification of *CDR2L* was found in 1 of 15 (6.6%) control samples ($p < 0.0001$). Of note, *CDR2L* and *ErbB2* both are on 17q chromosome, but, when associated, amplifications of both genes were not dependent on the same amplicon. Information on *CDR2* CNV was available for 10 samples by CGHa: 3 patients had a significant gain, but no amplification of this gene was found. Overall, all included patients with Yo-PCD had at least 1 BC sample harboring at least 1 alteration in *CDR2* or *CDR2L*: mutations (62.5%), amplifications (61.5%), or gains (38.4%) irrespective of the tumor site (primary tumor or metastasis). These alterations concerned only *CDR2L* for 9

of 14 samples (64.3%), both *CDR2L* and *CDR2* in 3 of 14 (21.4%), and *CDR2* alone in 2 of 14 (14.3%). RNA sequencing analysis found no differential expression of *CDR2* but confirmed significant overexpression of *CDR2L* transcript in Yo-PCD BCs compared with control BCs (Figure 2C). This high *CDR2L* antigen expression was confirmed at the protein level by IHC staining (Figure 2D) in Yo-PCD BCs vs matched controls ($p = 0.02$). All BCs with an amplification of *CDR2L* had a maximum staining intensity (3) on IHC, and 2 of 3 of those with gains or strong gains had a high intensity level (2).

Yo-PCD BCs Have a Specific Transcriptomic Profile

To approach the question of key pathways involved in Yo-PCD pathophysiology, we first performed bulk tumor RNA-seq. Analysis of the differentially expressed genes found 615 upregulated and 54 downregulated genes in Yo-PCD BCs (n = 12; 8 patients) compared with matched control BCs without PCD (n = 15; Figure 3A, adjusted *p*-value threshold = 0.01; log2FC threshold = 1). An exhaustive list of differentially expressed genes is available in eTable 1 (links.lww.com/NXI/A734). Hierarchical clustering based on the RNA expression profile of the 669 differentially expressed genes separates the samples into 2 main clusters: Yo-PCD BC samples including both primary (n = 9) and metastatic (n = 3) sites on one side and HER2-driven matched control BC samples on the other side. A core set of genes was constantly downregulated in Yo-PCD BCs, making it a putative hallmark of Yo-PCD transcriptomic profiles (Figure 3A). Functional GO enrichment analysis on this downregulated cluster found a predominance of extracellular matrix (ECM)-related genes, whereas overexpressed genes were mainly related to adaptive immune activation. Detailed GO enrichment analysis is provided in eTable 2 and eTable 3 (links.lww.com/NXI/A734).

Yo-PCD BCs Are Distinguished by Their Immune Cell Infiltration

GO enrichment analysis on overexpressed genes found an enrichment in B-cell and T-cell activation and proliferation pathways and adaptive immune response final pathways in Yo-PCD BCs (eTable 2 and eTable 3, links.lww.com/NXI/A734). The striking proportion of immune-related gene overexpression suggested a massive infiltration by immune cells in Yo-PCD compared with controls. To further analyze and quantify the implicated cell populations, we conducted an MCP-counter analysis exclusively on primary BCs in both groups. As expected, we found no difference in innate immunity components (neutrophils, NK cells, and monocytic lineage; Figure 3B). Analysis of B lineage and T cells revealed a strong intersample variability in Yo-PCD BCs. Three samples (1A, 1B, and 13A) had both low T-cell and B-cell counts and corresponded to samples of patients with another prevalent tumor (namely, 1C and 13B) with a higher MCP-score of adaptive immune cells. Indeed, a markedly elevated B- and/or T-cell MCP-score is found in the remaining 6 samples, probably accounting for the aforementioned adaptive immune pathway enrichment. However, all Yo samples, irrespective of their B- and T-cell MCP-score, were characterized by a significant overexpression of plasma cells/plasma blast genes (MZB1 and TNFRSF17; Figure 3C), suggesting that the latter cells may have a pivotal role in this strong adaptive immune reaction in Yo-PCD BCs.

An IgG-Plasma Cell Attack Characterizes Yo-PCD HER2-Driven BCs

Seven-color IF staining and digital image analysis were used to quantify tumor-infiltrating T cells, B cells, myeloid dendritic cells (mDCs), and IgG- and IgA-plasma cells in patients with available primary FFPE tumor tissue. These found a clearly more intense and diffuse infiltration by a wide variety of immune cells within and around the tumor tissue of Yo-PCD BCs compared with HER2-driven controls (Figure 4A) and confirmed the considerable proportion of IgG plasma cells in Yo-PCD BCs. Indeed, the median density (number of cells/mm^2) of T cells (CD3; Figure 4B) and mDC (DC-LAMP, data not shown) did not significantly differ between Yo and controls, whereas CD20 + B cells and most prominently IgG (but not IgA) plasma cell densities were significantly higher in Yo-PCD BCs compared with controls (Figure 4C and D).

Discussion

In our understanding of immune tolerance breakdown leading to paraneoplastic neurologic diseases, genetic alterations of onconeural antigens stand as a key element. Here, as in Yo-PCD ovarian cancer,[7] nearly two-thirds of the patients with Yo-PCD with a BC presented with at least 1 somatic alteration of a Yo gene, although alterations of these genes are very rare in BCs, including in HER2-positive ones, according to COSMIC database (<1%).[19] Although somatic mutations were also described in Yo ovarian cancers,[7] none was common to BCs and ovarian cancers, but all mutations have direct consequences on the corresponding protein and are thus likely to generate neoepitopes. However, this scenario of neoantigen creation does not fully apply to each Yo-PCD BC in this study. In that respect, gain in copy number leading to onconeural antigen overexpression itself may be a sufficient trigger for the occurrence of an immune tolerance breakdown, irrespective of the creation of neoepitopes, as it has been suggested by others concerning paraneoplastic anti-THSD7A membranous nephropathy.[20] Amplification (≥6 copies) mainly concerned *CDR2L*, and it was demonstrated herein that these *CDR2L* amplifications result in *CDR2L* transcript and protein overexpression in Yo-PCD BCs. Conversely, there were only infrequent copy number gains (<6) for *CDR2*, and these did not produce any detectable increase of *CDR2* expression. Thus, as already highly suspected,[21] the data presented herein support that CDR2L could be the major antigen in Yo-PCD, irrespective of the nature of the associated tumor. Yet, if strong similarities exist between Yo-PCD ovarian tumors and BCs, from the frequency of Yo genetic alteration to the intensity of the intratumor immune attack,[7] 2 specificities of Yo BCs suggest mechanistic differences in the immune tolerance breakdown triggering PCD between these 2 tumor types. First,

CDR2L amplification seems to be pivotal in Yo-PCD BCs, whereas ovarian Yo-PCD cancers only present gain in copy number. Second, as previously described,[8] a strong overrepresentation of HER2-positive BCs harboring both *ERBB2* gene amplification and HER2 overexpression in Yo-PCD BCs was found herein, whereas Yo-PCD ovarian cancers do not display *ERBB2* amplification.[7] Although *ERBB2* and *CDR2L* are located at the same chromosomic region (17q21-25), *CDR2L* amplification does not seem to be a consequence of *ERBB2* amplification, and FISH analysis ruled out double-minute chromosome; hence, the mechanism of this double amplification remains elusive. Further studies are needed to decipher this mechanism, as well as the interactions of these 2 proteins in PCD pathogenesis in Yo-PCD BCs, which are not only HER2-positive but also HR-negative invasive carcinomas of NST. This HER2-driven histopathologic signature is otherwise very marginally represented among BCs (around 3.2%),[22] which makes it a hallmark of Yo-PCD BCs. From a clinical perspective, HER2 negativity should thus raise suspicion of an alternative tumor site in the diagnostic workup for the underlying neoplasm in Yo-PCD. From a mechanistic perspective, this HER2-driven signature of Yo-PCD BCs is most probably implicated in the peculiar immune attack characterizing these BCs; several studies have described an overrepresentation of tumor-invasive CD4$^+$ and CD8$^+$ T cells and B cells in HR-negative BCs.[23-25] A potential explanation for this extraimmunogenic feature lies in the mutational load (number of somatic mutations per tumor), which is substantially higher in HR-negative than in HR-positive BCs[26] and mirrors the neoantigen load. The implication of HER2 positivity per se in tumor immunogenicity is, for its part, still elusive. But beyond this HER2-driven feature, other mechanisms might support Yo-PCD development because the tumors investigated herein presented a markedly more intense immune infiltration compared with HER2-driven controls. The most overrepresented immune cells were IgG-plasma cells suggesting the prominence of humoral immune attack in Yo-PCD BCs, probably linked with the production of Yo autoantibodies. This may also be related to a potential earlier diagnosis of Yo BCs allowing to capture the early phenomenon of the immune attack, although the equivalent tumor size distribution between Yo and control BCs pleads for the equivalent time of evolution. Taken together, this suggests that immune cells participate in an effective antitumor attack; however, as functional aspects could not be analyzed herein because retrospective collection can only concern fixed samples, it is also possible that these cells or a subset of these are exhausted. This is supported by the overwhelming proportion of lymph node–positive BCs among Yo-PCD BCs (80% vs 43% in HER2-driven BC series with a similar tumor size distribution),[27] implying that cancer cell migration escapes from immune surveillance. Even more striking is that more than a fifth of patients with Yo-PCD had OBC, whereas such a situation is rare in the general population of patients with BC (prevalence estimated to be 0.1%).[28] Considering OBC, HER2 positivity and HR negativity are 2 known risk factors, but, taken together, HER2-driven BC is only slightly overrepresented in OBC cohorts (3.1% in OBC vs 2.3% in non-OBC in the study reported in reference 29). Isolated DCIS concomitant to lymph node metastasis is another rarity (4.4% of DCIS),[30] not so infrequent in the present cohort of Yo-PCD BCs (2/3 DCIS with lymph node metastasis). Taken together, this suggests that Yo-PCD BCs show a strong and early propensity for lymphatic metastasis in their lifespan. In practice, awareness about this peculiar behavior of Yo-PCD BCs is critical to optimize the search for the underlying tumor: axillary lymph nodes should be promptly analyzed even without evidence of ipsilateral BCs. Such regression of the primary tumor (occult primary tumor) with concomitant lymph node metastasis is regularly described in melanoma and interpreted as the result of an effective past immune attack of the primary site.[31] A particularity of Yo-PCD BCs is the concomitant observation of an intense intratumor immune response and early metastasis, which is not described in regressive melanomas.[31] This could suggest that tumor microenvironment is particularly permissive to tumor cell migration in Yo-PCD BCs that may be related to the underexpression of ECM compounds characterizing Yo-PCD BC transcriptomic profiles.

Conclusion

This study indicates that there is a morphophenotypical signature of Yo-PCD BCs: invasive HER2-driven carcinoma overexpressing mutated *CDR2L* and metastasizing early to regional lymph nodes despite massive infiltration by effector immune cells with an overwhelming predominance of IgG-plasma cells. This specific BC profile, closely linked to HER2-driven carcinogenesis, undoubtedly participates in triggering the immune tolerance breakdown, leading to Yo-PCD autoimmunity.

Disclosure
The authors report no disclosures relevant to the manuscript. Go to Neurology.org/NN for full disclosures.

Appendix Authors

Name	Location	Contribution
Elise Peter, MSc	Synaptopathies and Autoantibodies (SynatAc) Team, Institut NeuroMyoGène-MeLiS, INSERM U1314/CNRS UMR 5284, Université de Lyon; French Reference Center on Paraneoplastic Neurological Syndrome, Hospices Civils de Lyon; University of Lyon, Université Claude Bernard Lyon 1, France	Drafting/revision of the manuscript for content, including medical writing for content; major role in the acquisition of data; and analysis or interpretation of data
Isabelle Treilleux, MD, PhD	Department of Biopathology, Centre Leon Berard, Lyon, France	Major role in the acquisition of data and analysis or interpretation of data
Valentin Wucher, PhD	University of Lyon, Université Claude Bernard Lyon 1; INSERM 1052, CNRS 5286, Centre Leon Berard, Centre de Recherche en Cancérologie de Lyon, France	Drafting/revision of the manuscript for content, including medical writing for content, and analysis or interpretation of data
Emma Jougla, MSc	University of Lyon, Université Claude Bernard Lyon 1; INSERM 1052, CNRS 5286, Centre Leon Berard, Centre de Recherche en Cancérologie de Lyon, France	Major role in the acquisition of data
Alberto Vogrig, MD	Synaptopathies and Autoantibodies (SynatAc) Team, Institut NeuroMyoGène-MeLiS, INSERM U1314/CNRS UMR 5284, Université de Lyon; French Reference Center on Paraneoplastic Neurological Syndrome, Hospices Civils de Lyon; University of Lyon, Université Claude Bernard Lyon 1, France	Drafting/revision of the manuscript for content, including medical writing for content
Daniel Pissaloux, PhD	Department of Biopathology, Centre Leon Berard; Cancer Genomics Platform, Department of Translational Research, Centre Leon Berard, Lyon, France	Major role in the acquisition of data
Sandrine Paindavoine, PhD	Department of Biopathology, Centre Leon Berard; Cancer Genomics Platform, Department of Translational Research, Centre Leon Berard, Lyon, France	Major role in the acquisition of data
Justine Berthet, MSc	Department of Biopathology, Centre Leon Berard; Cancer Genomics Platform, Department of Translational Research, Centre Leon Berard; Laboratoire d'Immunothérapie des Cancers de Lyon (LICL), France	Major role in the acquisition of data

Appendix (continued)

Name	Location	Contribution
Géraldine Picard	French Reference Center on Paraneoplastic Neurological Syndrome, Hospices Civils de Lyon, France	Major role in the acquisition of data
Véronique Rogemond, PhD	University of Lyon, Université Claude Bernard Lyon 1; INSERM 1052, CNRS 5286, Centre Leon Berard, Centre de Recherche en Cancérologie de Lyon, France	Major role in the acquisition of data
Marine Villard	French Reference Center on Paraneoplastic Neurological Syndrome, Hospices Civils de Lyon, France	Major role in the acquisition of data
Clémentine Vincent, PhD	University of Lyon, Université Claude Bernard Lyon 1; INSERM 1052, CNRS 5286, Centre Leon Berard, Centre de Recherche en Cancérologie de Lyon, France	Major role in the acquisition of data
Laurie Tonon, PhD	Synergie Lyon Cancer-Bioinformatics Platform-Gilles Thomas, Centre de Recherche en Cancérologie de Lyon	Analysis or interpretation of data
Alain Viari, PhD	Synergie Lyon Cancer-Bioinformatics Platform-Gilles Thomas, Centre de Recherche en Cancérologie de Lyon	Analysis or interpretation of data
Jérôme Honnorat, MD, PhD	Synaptopathies and Autoantibodies (SynatAc) Team, Institut NeuroMyoGène-MeLiS, INSERM U1314/CNRS UMR 5284, Université de Lyon; French Reference Center on Paraneoplastic Neurological Syndrome, Hospices Civils de Lyon; University of Lyon, Université Claude Bernard Lyon 1, France	Drafting/revision of the manuscript for content, including medical writing for content; study concept or design; and analysis or interpretation of data
Bertrand Dubois, PhD	INSERM 1052, CNRS 5286, Centre Leon Berard, Centre de Recherche en Cancérologie de Lyon; Laboratoire d'Immunothérapie des Cancers de Lyon (LICL), France	Drafting/revision of the manuscript for content, including medical writing for content; study concept or design; and analysis or interpretation of data
Virginie Desestret, MD, PhD	Synaptopathies and Autoantibodies (SynatAc) Team, Institut NeuroMyoGène-MeLiS, INSERM U1314/CNRS UMR 5284, Université de Lyon; French Reference Center on Paraneoplastic Neurological Syndrome, Hospices Civils de Lyon; University of Lyon, Université Claude Bernard Lyon 1, France	Drafting/revision of the manuscript for content, including medical writing for content; study concept or design; and analysis or interpretation of data

References

1. Furneaux HF, Reich L, Posner JB. Autoantibody synthesis in the central nervous system of patients with paraneoplastic syndromes. *Neurology* 1990;40(7):1085-1085.

2. Peterson K, Rosenblum M, Kotanides H, Posner J. Paraneoplastic cerebellar degeneration.: IA clinical analysis of 55 anti-Yo antibody-positive patients. *Neurology* 1992;42(10):1931-1931.

3. Verschuuren J, Chuang L, Rosenblum MK, et al. Inflammatory infiltrates and complete absence of Purkinje cells in anti-Yo-associated paraneoplastic cerebellar degeneration. *Acta Neuropathol (Berl)* 1996;91(5):519-525.

4. Darnell JC, Albert ML, Darnell RB. Cdr2, a target antigen of naturally occurring human tumor immunity, is widely expressed in gynecological tumors. *Cancer Res* 2000;60(8):2136-2139.

5. Eichler TW, Totland C, Haugen M, et al. CDR2L antibodies: a new player in paraneoplastic cerebellar degeneration. *PLoS One* 2013;8(6):e66002.

6. Totland C, Aarskog NK, Eichler TW, et al. CDR2 antigen and Yo antibodies. *Cancer Immunol Immunother* 2011;60(2):283-289.

7. Small M, Treilleux I, Couillault C, et al. Genetic alterations and tumor immune attack in Yo paraneoplastic cerebellar degeneration. *Acta Neuropathol (Berl)* 2018;135(4):569-579. doi: 10.1007/s00401-017-1802-y

8. Rojas-Marcos I, Picard G, Chinchón D, et al. Human epidermal growth factor receptor 2 overexpression in breast cancer of patients with anti-Yo–associated paraneoplastic cerebellar degeneration. *Neuro-Oncol.* 2012;14(4):506-510.

9. Graus F, Vogrig A, Muñiz-Castrillo S, et al. Updated diagnostic criteria for paraneoplastic neurologic syndromes. *Neurol - Neuroimmunol Neuroinflammation* 2021;8(4):e1014. doi: 10.1212/NXI.0000000000001014

10. WHO classification of tumours. Editorial board. Breast tumours. Lyon (France): IARC: 2019.(WHO classification of tumours series 5th Ed; Vol 2). 5th ed.

11. Dobin A, Davis CA, Schlesinger F, et al. STAR: ultrafast universal RNA-seq aligner. *Bioinformatics* 2013;29(1):15-21.

12. Broad Institute. *Picard Toolkit*; 2019. broadinstitute.github.io/picard/.

13. R Development Core Team. *R: A Language and Environment for Statistical Computing*. R Foundation for Statistical Computing. R foundation for Statistical Computing; 2010. R-project.org.

14. Love MI, Huber W, Anders S. Moderated estimation of fold change and dispersion for RNA-seq data with DESeq2. *Genome Biol* 2014;15(12):1-21.

15. Gu Z, Eils R, Schlesner M. Complex heatmaps reveal patterns and correlations in multidimensional genomic data. *Bioinformatics* 2016;32(18):2847-2849.

16. Yu G, Wang LG, Han Y, He QY. clusterProfiler: an R package for comparing biological themes among gene clusters. *Omics J Integr Biol* 2012;16(5):284-287.

17. Becht E, Giraldo NA, Lacroix L, et al. Estimating the population abundance of tissue-infiltrating immune and stromal cell populations using gene expression. *Genome Biol* 2016;17(1):1-20.

18. Galea MH, Blamey RW, Elston CE, Ellis IO. The Nottingham Prognostic Index in primary breast cancer. *Breast Cancer Res Treat* 1992;22(3):207-219.

19. Tate JG, Bamford S, Jubb HC, et al. COSMIC: the catalogue of somatic mutations in cancer. *Nucleic Acids Res* 2019;47(D1):D941–D947.

20. Hoxha E, Wiech T, Stahl PR, et al. A mechanism for cancer-associated membranous nephropathy. *N Engl J Med* 2016;374(20):1995.

21. Kråkenes T, Herdlevær I, Raspotnig M, Haugen M, Schubert M, Vedeler CA. CDR2L is the major Yo antibody target in paraneoplastic cerebellar degeneration. *Ann Neurol* 2019;86(2):316-321.

22. van Dooijeweert C, Deckers IAG, Baas IO, van der Wall E, van Diest PJ. Hormone- and HER2-receptor assessment in 33,046 breast cancer patients: a nationwide comparison of positivity rates between pathology laboratories in the Netherlands. *Breast Cancer Res Treat* 2019;175(2):487-497. doi: 10.1007/s10549-019-05180-5

23. Cheung YC, Chen SC, Su MY, et al. Monitoring the size and response of locally advanced breast cancers to neoadjuvant chemotherapy (weekly paclitaxel and epirubicin) with serial enhanced MRI. *Breast Cancer Res Treat* 2003;78(1):51-58.

24. Garaud S, Buisseret L, Solinas C, et al. Tumor infiltrating B-cells signal functional humoral immune responses in breast cancer. *JCI Insight* 2019;5(18):e129641. doi: 10.1172/jci.insight.129641

25. Kim M, Chung YR, Kim HJ, Woo JW, Ahn S, Park SY. Immune microenvironment in ductal carcinoma in situ: a comparison with invasive carcinoma of the breast. *Breast Cancer Res BCR* 2020;22(1):32-32. doi: 10.1186/s13058-020-01267-w

26. Luen S, Virassamy B, Savas P, Salgado R, Loi S. The genomic landscape of breast cancer and its interaction with host immunity. *The Breast* 2016;29:241-250. doi: 10.1016/j.breast.2016.07.015

27. Dihge L, Vallon-Christersson J, Hegardt C, et al. Prediction of lymph node metastasis in breast cancer by gene expression and clinicopathological models: development and validation within a population-based cohort. *Clin Cancer Res* 2019;25(21):6368-6381.

28. Walker GV, Smith GL, Perkins GH, et al. Population-based analysis of occult primary breast cancer with axillary lymph node metastasis. *Cancer* 2010;116(17):4000-4006.

29. Ge LP, Liu XY, Xiao Y, et al. Clinicopathological characteristics and treatment outcomes of occult breast cancer: a SEER population-based study. *Cancer Manag Res* 2018;10:4381.

30. Yonekura R, Osako T, Iwase T, et al. Prognostic impact and possible pathogenesis of lymph node metastasis in ductal carcinoma in situ of the breast. *Breast Cancer Res Treat* 2019;174(1):103-111.

31. Alquier-Bouffard A, Franck F, Joubert-Zakeyh J, et al. [Regression in primary cutaneous melanoma is not predictive for sentinel lymph node micrometastasis]. *Ann Dermatol Venereol* 2007;134(6-7):521-525. doi: 10.1016/s0151-9638(07)89262-3

Immune and Genetic Signatures of Breast Carcinomas Triggering Anti-Yo–Associated Paraneoplastic Cerebellar Degeneration

Elise Peter, Isabelle Treilleux, Valentin Wucher, et al.

This information is current as of July 12, 2022

Updated Information & Services	including high resolution figures, can be found at: http://nn.neurology.org/content/9/5/e200015.full.html
References	This article cites 28 articles, 5 of which you can access for free at: http://nn.neurology.org/content/9/5/e200015.full.html##ref-list-1
Permissions & Licensing	Information about reproducing this article in parts (figures,tables) or in its entirety can be found online at: http://nn.neurology.org/misc/about.xhtml#permissions
Reprints	Information about ordering reprints can be found online: http://nn.neurology.org/misc/addir.xhtml#reprintsus

AMERICAN ACADEMY OF
NEUROLOGY®